WATER RESOURCES RESEARCH, VOL. 31, NO. 1, PAGES 19–26, JANUARY 1995

Early development of karst systems
2. Turbulent flow

Alan D. Howard and Christopher G. Groves[1]
Department of Environmental Sciences, University of Virginia, Charlottesville

Abstract. A simulation model developed to explore patterns of fracture enlargement within incipient limestone karst aquifers has been extended to turbulent flow. In contrast to the highly selective passage enlargement that occurs early in cave network development under laminar flow, the transition to turbulent flow results in more general passage enlargement, leading to maze networks when initial fractures are large and hydraulic gradients are high. These results support previously published hypotheses for the development of maze patterns, including formation within structural settings that have created initially large fractures or within flow systems periodically inundated by flooding. Maze development is also favored under turbulent flow when passages are entirely water filled, and where the groundwater flow system is long-lived. By contrast, branched patterns are most common when passages become free-surface subterranean streams, because depression of the piezometric surface along main passages, downcutting along main passages, and possible infilling with sediment of side passages limit the sharing of discharge among interconnected fractures or bedding planes that promote maze development.

Introduction

A major question concerning pattern development of karst flow systems concerns the selective enlargement, or lack thereof, among a large number of potential flow paths along fractures or bedding planes within a body of limestone making up an incipient karst aquifer. Geologic and hydrochemical controls on the development of these patterns have been studied using both field observations and quantitative analyses [e.g., *Davis*, 1930; *Bretz*, 1942; *Dieke*, 1960; *White and Longyear*, 1962; *Howard*, 1963, 1964; *Curl*, 1974; *Palmer*, 1975, 1984, 1991; *Powell*, 1977; *White*, 1977, 1988; *Ford and Ewers*, 1978; *Ford and Williams*, 1989; *Sasowsky*, 1992]. This paper is the second devoted to a quantitative analysis of the conditions that lead to selective (single-passage or branched) versus nonselective (maze) flow path development during the earliest stages of karst flow system evolution.

Such an analysis is complicated by the dependency of the rate of limestone dissolution upon both chemical and hydrodynamic conditions within the fluid forming the system [*Plummer and Wigley*, 1976; *White*, 1988; *Dreybrodt*, 1988, 1990; *Palmer*, 1991], both of which are constantly changing as system evolution proceeds. As a consequence, simulation modeling is the most practical approach to investigating early stages of limestone aquifer development. This paper extends our model for solution within fracture systems under laminar flow [*Groves and Howard*, 1994b] to the turbulent flow that occurs during later stages of passage enlargement.

[1]Now at Center for Cave and Karst Studies, Department of Geography and Geology, Western Kentucky University, Bowling Green.

Paper number 94WR01964.
0043-1397/95/94WR-01964$05.00

Model Structure

Natural fracture systems in limestone are represented in the model by networks of cylindrical pipes which are then subjected to dissolution. Several configurations have been utilized, including single recharge and exit locations, multiple recharge sources, and multiple exits. Justification for use of pipes rather than parallel-walled fractures is presented by *Groves and Howard* [1994b].

At each time step and at each location within the network of passages, three potential rate-limiting kinetic mechanisms are evaluated. These are surface reactions at the limestone-water interface (reaction-limited rate), mass transfer of calcium ions from the limestone surface to the bulk solution (transfer-limited rate), and CO_2 hydration in the bulk solution (hydration-limited rate). The actual dissolution rate becomes the minimum among these rate-limiting processes. The *Palmer* [1991] surface reaction rate law, which is based upon an empirical analysis of data from *Plummer and Wigley* [1976] and *Plummer et al.* [1978] on dissolution rates R (L/T) in the calcite-CO_2-water system as a function of the saturation deficit s and a rate constant k (L/T), is used in this paper

$$R = ks^n, \tag{1}$$

where

$$s = (1 - C/C_s). \tag{2}$$

The reaction-limited rate is divided into low-order kinetics (n_1 and k_1) for when the solution is less than a critical saturation deficit s_c and a high-order rate (n_2, k_2) for $s > s_c$. The transfer-limited rate is assumed to be controlled by calcium ion migration, with diffusion control under laminar flow [*Groves and Howard*, 1994a], whereas under turbulent flow the convection correlation of *Gnielinski* [1976] is uti-

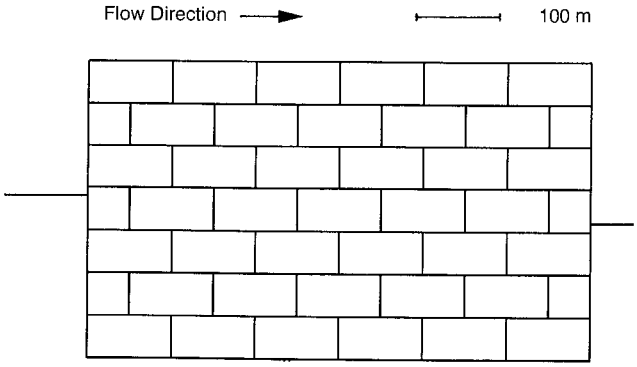

Figure 1. Map of model conduit network. In this and all other figures flow is from left to right. All passages are fluid filled, and network can be considered to be oriented vertically or horizontally.

lized. Details of the dissolution model have been described elsewhere [*Groves*, 1993; *Groves and Howard*, 1994a, b].

Each of the interconnected pipes in the idealized networks (e.g., Figure 1) is composed of a series of short "elements," generally 1 m in length, so that each pipe has 50–150 component elements. The exception is pipes at flow entrances where pipes have 1000 elements whose lengths follow a logistical equation [*Groves and Howard*, 1994b] with very short elements (approximately 10^{-4} m) at the very entrance where the solution chemistry in laminar flow changes rapidly downstream. Groundwater chemical evolution and passage dissolution are calculated individually for each element. However, elements within a given pipe are lumped using an effective diameter (discussed below) for network flow calculations.

Flow in the pipe networks is assumed to be fully developed and incompressible and to have constant fluid viscosity and density. Head losses as a result of passage constrictions, expansions, and bends are assumed to be negligible. The passages are assumed to be fully filled with groundwater (phreatic conditions).

A basic network of 146 conduits was implemented in this study (Figure 1), although there is no inherent limitation of the model to a two-dimensional space. The conduit system can be visualized to be oriented either in the vertical or horizontal plane; however, in the former case, passages are assumed to remain water filled. The hydraulic head at exit points is specified and unchanging during the simulation. Two end-member boundary conditions at recharge entrances were imposed. Heads either remain fixed throughout the simulation or decline after a designated maximum discharge value is reached. The former corresponds to an excess of available supply of surface water at flow entrances and would typically occur during very early stages of cavern development. The fixed maximum discharge corresponds to a situation where there is a limited available recharge from the surface (from sinkholes or sinking streams) but hydrogeologic relations keep the entire network flooded (as in the case of artesian groundwater flow through limestones).

Under laminar flow conditions a set of linear equations relating discharges and head losses within the network can be written and readily solved [*Groves and Howard*, 1994b]. However, in turbulent flow the relationship is nonlinear, so that alternative techniques must be used to solve for the flow field. The approach adopted here utilizes a system of linearized equations of mass conservation for discharge at each passage junction (node) with the head losses through the pipes entering each node as unknowns:

$$\sum Q_{ij} = \sum \frac{(H_i - H_j)}{K_{ij}} = Q_r \tag{3}$$

where Q_{ij} is the discharge entering or exiting the local node j from passages leading to adjacent nodes i, Q_r is recharge or discharge (only nonzero at flow entrance and exit locations), H_i is the head at adjacent nodes, and K_{ij} are coefficients. Flow resistance in tubes is generally specified by a friction factor f:

$$\Delta H = \frac{fLV^2}{2gD_e} = \frac{8fLQ^2}{\pi^2 D_e^5 g} \tag{4}$$

where L is the conduit length, D_e is the effective conduit diameter (see below), V is mean velocity, ΔH is the head loss through the tube, and g is gravitational acceleration. For laminar flow,

$$f = 64/R = 64\nu/VD_e = 16\pi\nu D_e/Q \tag{5}$$

where R is the Reynolds number and ν is kinematic viscosity. Thus for laminar flow the coefficients K in (3) depend only on passage length and diameter:

$$K = 128\nu L/\pi g D_e^4 \tag{6}$$

so that the system of equations (3) is linear. However, in transitional and turbulent flow f depends upon the Reynolds number in a complicated fashion. This is simplified in the present model by considering only two turbulent regimes, hydraulically smooth and fully rough. For hydraulically smooth flow,

$$f = 0.316/R^{0.25} \tag{7}$$

and for fully rough flow,

$$f = 1/[1.14 - 2\log_{10}(e/D_e)]^2 \tag{8}$$

where e is the roughness length [*Jeppson*, 1976]. For turbulent flow when (7) or (8) is substituted into (4) and (3) the coefficients K depend upon discharge. Any of laminar, rough-turbulent, and smooth-turbulent flow may occur within different passages in a cave network, so that the relationship between the heads and discharges in (3) is nonlinear.

The approach adopted here to solve equations (3) for the unknown heads at nodes is to assign initial values to the K coefficients, and to iterate toward the correct solution by using the estimated discharges to improve estimates of the coefficients, as described by *Jeppson* [1976]. For each iteration the equations (3) are solved by lower-upper (LU) decomposition with iterative improvement using routines from *Press et al.* [1986].

Within each pipe the appropriate friction factor is determined during each iteration by calculating the Reynolds number. If R is less than a critical value $R_t = 2300$, then (5) is used. For $R > R_t$ then the maximum f among (6) and (7) is used. Because of the jump of friction factor at the threshold of turbulence, the solution may fail to converge because successive iterations result in alternating turbulent

Table 1. Input Parameters and Calculated Flow and Geometric Conditions for Simulations

	Run							
	1	2	3	4	5	6	7	8
Initial passage diameter, m	0.01	0.001	0.01	0.01	0.001	0.01	0.001	0.001
Initial head difference, m	0.25	5.0	0.25	0.2	5.0	0.2	5.0	40.0
Initial exit discharge, m^3/s	2.23×10^{-6}	5.43×10^{-9}	2.23×10^{-6}	2.83×10^{-6}	9.92×10^{-9}	2.89×10^{-6}	9.92×10^{-9}	7.94×10^{-8}
Maximum recharge rate, m^3/s	...	...	0.1	...	...	0.01	0.01	0.01
Final exit discharge, m^3/s	5.63	17.0	0.1	5.64	12.81	0.06	0.06	0.06
Maximum final effective diameter, m	1.99	2.24	2.26	2.04	2.94	1.99	2.09	2.45
Final elapsed time, years	780	86,820	850	1,800	109,000	2,359	109,600	7,131
Final maze index (I_m)	10.5	1.2	4.3	11.1	1.3	5.8	2.3	2.9

and laminar flow. To avoid this, a hysteresis was introduced such that the transition from turbulent to laminar flow occurs at $R = 0.3R_t$. Because enlarging passages that change from laminar to turbulent flow seldom subsequently revert to laminar flow, changing the value of the laminar-turbulent transition has little effect on the predicted pattern or elapsed time of passage development. The effect of variation of R_t on simulated cave development is discussed later.

For flow solutions that occur after the first pass of water through the network, and thus after individual pipes have nonuniform diameters due to solutional enlargement, an "effective diameter," D_e, is calculated for each pipe for use in (4)–(8). This is the diameter for a uniform pipe that experiences the same head loss as the actual sequence of element diameters:

$$D_e = \left[\sum L_i \Big/ \sum (L_i/D_i^4) \right]^{1/4} \tag{9}$$

where the L_i and D_i are length and diameter values for individual elements. This calculated effective diameter is exact only for passages with laminar flow, because the relationship between head loss and diameter is different for turbulent flow; equation (9) is used for computational efficiency, and it gives a sufficiently accurate estimate of D_e for turbulent flow, because passage width generally varies only slowly downstream.

A set of nominal geometric and chemical parameters was chosen as follows: the total network runs 750 m left to right, and 350 m top to bottom, with all conduits having a specified uniform initial diameter; a head drop across the system is specified, and there may be a fixed maximum discharge; the wall roughness, e, is 0.0002 m; the fluid has an initial pCO_2 of 0.03 atm, a constant temperature of 15°C; and the flow system is closed with respect to the addition or loss of CO_2 gas. The surface reaction rate law of *Palmer* [1991] for pure limestone and $pCO_2 = 0.03$ atm is utilized, giving $n_1 = 1.7$, $n_2 = 4.0$, and $s_c = 0.7$. Runs were made with a variety of initial geometries and flow boundary conditions (Table 1).

Results

All of the simulations reported here start from an initial network of uniform-width passages under flow conditions that are initially laminar. As reported by *Groves and Howard* [1994b], dissolution during the initial laminar flow conditions is highly selective, such that only one flow path from each external recharge source to the exit spring is appreciably enlarged, leading to single-passage systems or, with multiple recharge locations, branched (dendritic) passages. Figure 2 shows the passage diameters for a typical simulation under fixed hydraulic head just before the transition to turbulent flow along the main passage. The width of the lines representing the passages is approximately proportional to effective diameter, D_e, of the passages. Note that passage diameters decrease downstream, approximately following a negative exponential function. For realistic initial hydraulic gradients ($H/L < 0.1$) the transition to turbulence within the main passage(s) occurs while the passage diameters are quite small (maximum approximately 0.07 m, average approximately 0.02 m), as are the discharges (approximately 4×10^{-6} m^3/s).

In this paper we present simulations in which turbulent

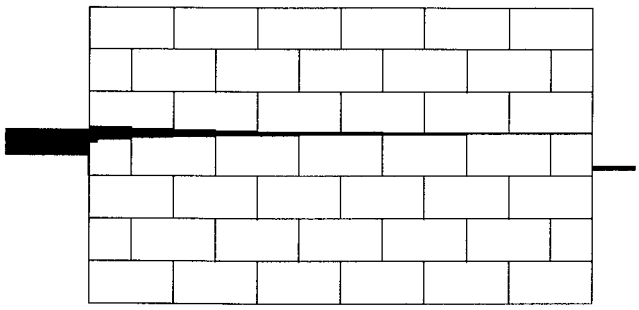

Figure 2. Effective passage diameters at onset of turbulence.

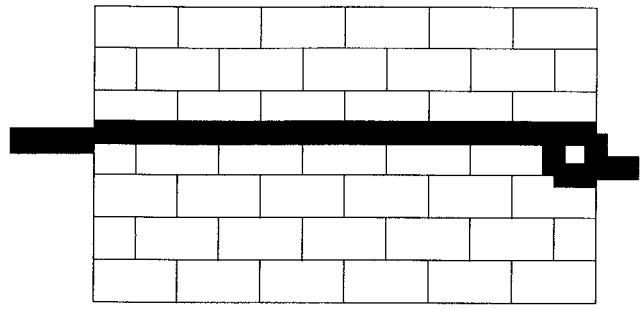

Figure 4. Final effective passage diameters for run 2.

flow is achieved in the major passages. All of the simulations are continued until the maximum effective passage diameter among recharge entrance tubes reaches about 2 m. Runs have been conducted for single and multiple recharge locations and for fixed head and fixed maximum discharge conditions.

Single Input, Fixed Input Head

Simulations have utilized a variety of initial passage diameters and various imposed heads at the recharge point. During turbulent flow the deep penetration of fresh solutions results in nearly uniform solution along the major flow paths, so that passage diameters are nearly constant downstream (run 1, Figure 3). Depending upon the initial passage diameter and imposed head, the resulting cave network varies from extremely mazelike (run 1, Figure 3) to essentially single-passage (run 2, Figure 4). In general, enlargement during turbulent flow is less selective than during laminar flow, with greater development of alternate flow paths. Two factors are responsible for the more mazelike development under turbulent flow:

1. The deep penetration of undersaturated solutions along the main passages permits rapid development of alternate flow paths fed from the main passages.
2. Under turbulent flow the greater rate of increase of frictional resistance with increase in flow rate as compared with laminar flow means that alternate flow paths with longer path lengths or smaller diameters receive a proportionately larger amount of flow than is the case for laminar flow; that is, flow is more evenly distributed within the network. The more equable sharing of flow is particularly marked when flow through the largest channel is turbulent and the alternate flow paths carry laminar flow.

Single Source, Fixed Maximum Discharge

Run 3 (Figure 5) is identical to run 1 except that a maximum discharge of 0.1 m^3/s is imposed. For this run the extent of maze development is considerably less than for the equivalent run with unconstrained discharge (run 1).

Multiple Sources, Fixed Input Head

A passage configuration with six input sources and one exit was selected. Figure 6 (run 4) shows the relative passage sizes at the initiation of turbulent flow and at the close of the simulation for a large initial passage diameter (0.01 m). The highly selective enlargement under laminar flow becomes replaced by much less selective maze development under turbulent flow. For a combination of much smaller initial diameter (0.001 m) and low hydraulic gradient (run 5, Figure 7), maze development is inhibited, and only a single passage from a single source becomes significantly enlarged.

Multiple Sources, Fixed Maximum Discharge

Figures 8 (run 6) and 9 (run 7) show passage development for fixed maximum discharge of 0.01 m^3/s corresponding to results for unconstrained discharge shown in Figures 6 and 7, respectively. For the case of the larger initial passage size (Figure 8), imposition of a fixed discharge diminishes maze development, as it did for a single input. However, in the case of small initial passage diameter, a fixed maximum discharge limits the rate of development of the most direct passage, allowing the other sources to partially catch up in solutional development, forming a branched pattern.

Rate Controlling Processes

Because of the slow flow rates occurring during the initial stages of cave development under laminar flow conditions, the groundwater approaches saturation within the first few centimeters or meters, and fourth-order surface reaction

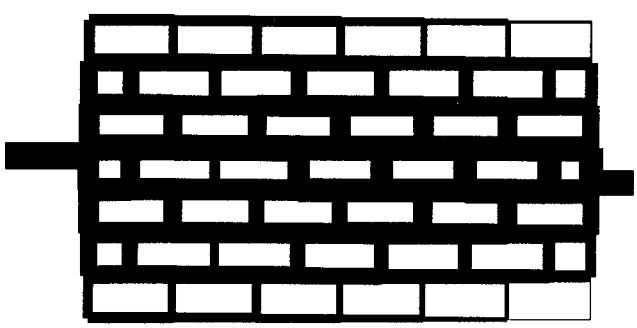

Figure 3. Final effective passage diameters for run 1.

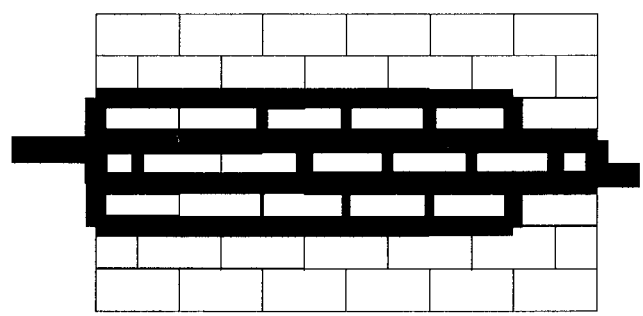

Figure 5. Final effective passage diameters for run 3.

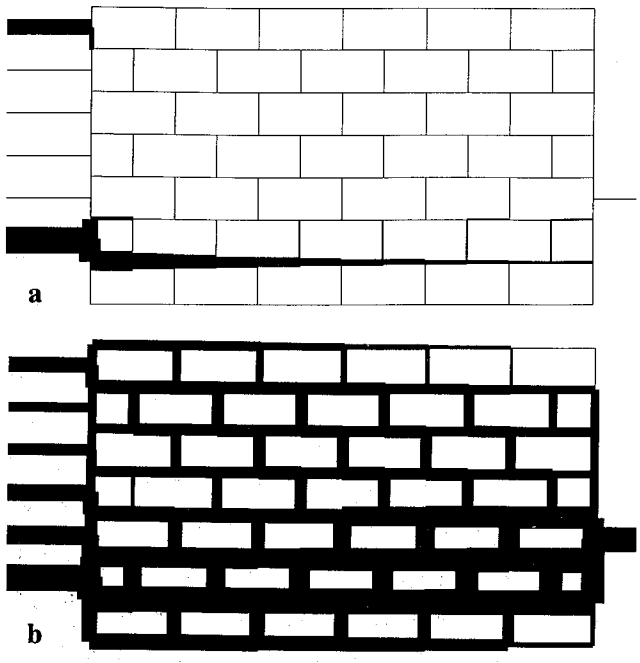

Figure 6. (a) Effective passage diameters at onset of turbulence for run 4. (b) Final effective passage diameters.

kinetics are the controlling factor throughout most of the network. Just before the transition to turbulence, dissolution in the main passages becomes controlled by laminar diffusion, whereas fourth-order surface reactions remain the limiting factor throughout the bulk of the network. As discussed by *White* [1977], *Dreybrodt* [1990], *Palmer* [1991], and *Groves and Howard* [1994a, b], the rate of dissolution in the main passage increases dramatically when enlargement becomes sufficient for high-order kinetics to no longer be the controlling kinetic factor. The transition to turbulence further increases the rate of dissolution because of the efficiency of turbulent convection, such that either turbulent convection or low-order surface reactions become the rate-controlling factor. During the final stages of solution within networks with fixed head, enlargement of the major passages is controlled by low-order surface reactions, whereas in passages with laminar flow, diffusional or the slower fourth-order surface reactions pertain. The pattern is different when a low maximum discharge is imposed, because turbulent convection becomes the controlling factor in the major passages due to the slow flow rates, whereas the minor passages continue to be dominated by either laminar diffusion or fourth-order kinetics. Hydration of CO_2 never becomes a rate-controlling process under the flow conditions considered in this paper.

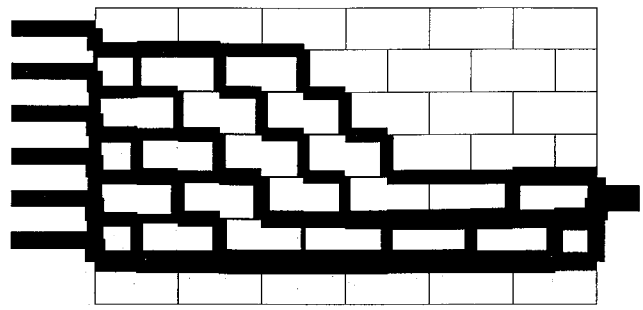

Figure 8. Final effective passage diameters for run 6.

The imposition of a maximum flow rate can have an important influence on passage development at locations where flow converges. Figure 10 (run 8) shows a network developed with multiple inputs with a small maximum discharge (0.01 m^3/s). The single passage in the interior of the cave system has been enlarged more than any of the entrance passages. This is because of the flow rate sensitivity of passage enlargement under turbulent convection; the combined flow along the main stem enlarges it faster. This pattern does not occur under fixed head conditions, because the low-order surface reaction kinetics that pertain are independent of flow rate.

Examination of a number of simulations with initial diameters ranging from 0.001 to 0.01 m and imposed heads from 40 to 0.25 m (including runs with fixed maximum discharge) reveals that the relative extent of maze development depends very strongly upon initial diameter and less strongly upon the initial head, with greatest maze development for the largest values of initial diameter and imposed hydraulic head. This would be expected from the greater influence upon flow rates in tubes of variations in passage diameter as compared to hydraulic gradient. This has been quantified by a "maze index," I_m, defined as the ratio of (1) the total length of passages with effective diameters greater than one tenth of the largest effective diameter within the network to (2) the minimum straight-line length of the cave from flow entrances to flow exit (750 m for the simulated networks). The maze index is greater than unity for the cave systems created by turbulent flow, but it is generally less than unity under laminar flow conditions because of the rapid downstream decrease in passage diameter. A regression of log-transformed variables for the maze index at the end of the

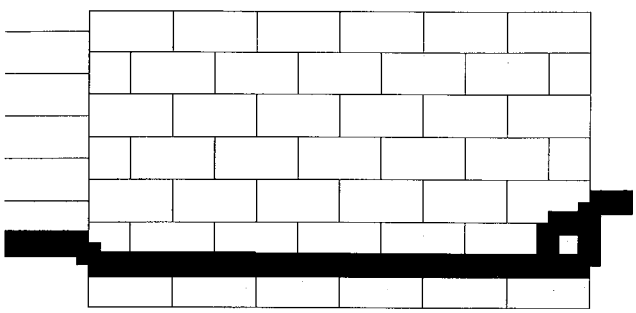

Figure 7. Final effective passage diameters for run 5.

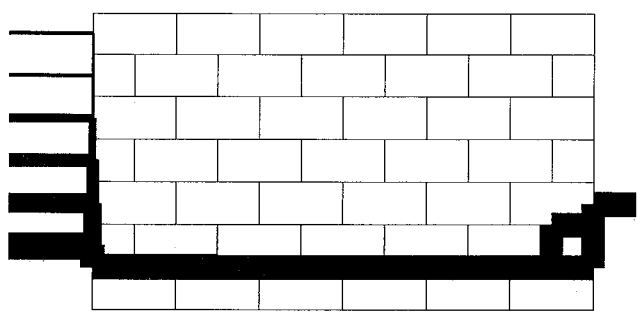

Figure 9. Final effective passage diameters for run 7.

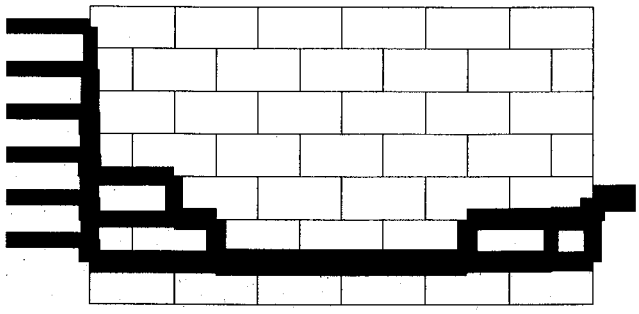

Figure 10. Final effective passage diameters for run 8.

runs for 12 simulations with six entrances and one exit (e.g., Figures 6–10) gives the following relationship:

$$I_m = 4.6 \times 10^4 D_e^{1.17} i^{0.36} (Q_m/Q_f)^{0.05} \quad (10)$$

where D_e is the initial effective passage diameter (meters), i is the initial maximum hydraulic gradient between flow entrance and exit ($\Delta H/L$), Q_m is the actual maximum recharge at the close of the simulation, and Q_f is the maximum recharge rate at the close of the simulation for an equivalent fixed head case. The ratio Q_m/Q_f equals unity for fixed head conditions, but is less than unity for a fixed maximum discharge. For example, for run 6 Q_f equals 0.01 (Table 1), and Q_m for the equivalent fixed head run (run 4) is 5.64 (Table 1). This relationship explains about 83% of the variance of I_m. Although specific coefficients are reported in (10) and Table 1, they should not be considered to be directly applicable to natural cave systems.

Sensitivity Analysis

The kinetics of calcite dissolution are somewhat uncertain, particularly the behavior close to saturation, where surface reaction rates diminish rapidly and are generally modeled by a high-order rate dependence upon saturation deficit. An initial passage diameter (0.001 m) and a single fixed entrance head (40 m) were used to investigate different rate law and boundary condition assumptions. These "nominal" conditions result in about half of the passages being enlarged into a maze (similar to run 3, Figure 5; Table 2).

Simulations were conducted varying the model parameters n_2 and s_c governing high-order surface reaction kinetics, the assumed Reynolds number R_t corresponding to the onset of turbulent flow, the wall roughness e, and the pCO_2 of the water at recharge locations (Table 2). For another run all passage lengths were doubled (except for the 100-m entrance tube) while maintaining the overall hydraulic gradient i and the same initial passage diameter ("double length" in Table 2).

Two published dissolution rate law models were utilized in addition to the *Palmer* [1991] surface reaction relationship used in this paper. *Plummer et al.* [1978] propose a four-term surface reaction kinetic model. One term depends upon surface pH; it is important only for low pH (highly undersaturated flows under turbulent flow) and is dependent upon hydrogen ion migration from the bulk solution. Runs were made with and without this term (Table 2); for the run ignoring this term the transfer-limited portion of the present model was assumed to be an approximate model of hydrogen ion mass transfer. The *Dreybrodt* [1990] fourth-order surface reaction model was assumed to approximate surface reaction kinetics for $s > 0.7$ for runs using the *Plummer et al.* [1978] rate law. Finally, the kinetic model of *Dreybrodt* [1990] was utilized for both low- and high-order surface kinetics and laminar diffusion for two assumed values of s_c. The *Gnielinski* [1976] relationship was utilized for turbulent convection for runs using both the *Plummer et al.* [1978] and *Dreybrodt* [1990] kinetic models (Table 2).

In general, the parameter and model variations have considerable effect on development time for equivalent stages of cave development, but very slight effect on the general pattern of high selectivity during enlargement under laminar flow and more uniform dissolution under turbulent flow (Table 2). Most of the resulting cave patterns are very similar, as indicated by very slight variations in the maze index, I_m. However, a greater degree of maze development occurs as pCO_2 increases, and doubling the cave size reduces the amount of maze development for equivalent hydraulic gradient and initial passage size. Furthermore, the *Dreybrodt* [1990] kinetic model predicts a greater degree of maze development, and less selectivity during laminar flow, than the *Palmer* [1991] and *Plummer et al.* [1978] models,

Table 2. Results of Sensitivity Analysis Runs

Rate Law	Changed Parameter	At Laminar-Turbulent Transition		At 1 m Maximum Diameter	
		Elapsed Time, years	Maze Index (I_m)	Elapsed Time, years	Maze Index (I_m)
Palmer [1991]	nominal run*	4,102	0.7	4,286	3.7
Palmer [1991]	R_t = 1000	4,096	0.6	4,346	3.7
Palmer [1991]	s_c = 0.9	10,325	0.5	10,539	3.0
Palmer [1991]	n_2 = 5.0	3,348	0.7	3,569	3.7
Palmer [1991]	n_2 = 3.0	2,096	0.7	6,856	3.2
Palmer [1991]	pCO_2 = 0.3 atm	175	1.3	250	6.5
Palmer [1991]	pCO_2 = 0.003 atm	22,600	0.9	23,176	1.4
Palmer [1991]	e = 0.0008 m	4,102	0.7	4,331	3.7
Palmer [1991]	double length	10,113	0.5	10,348	1.8
Dreybrodt [1990]	s_c = 0.7	1,415	1.5	2,158	4.8
Dreybrodt [1990]	s_c = 0.9	30,339	10.9	47,295	10.7
Plummer et al. [1978]	all terms	1,077	1.0	1,133	1.4
Plummer et al. [1978]	no H^+ term	1,068	0.8	1,372	4.5

*Initial passage diameter 0.001 m; initial head difference 40 m; initial pCO_2 = 0.03 atm; transition to turbulent flow at R_t = 2300; transition to high-order kinetics at s_c = 0.7; high-order exponent n_2 = 4.0; wall roughness e = 0.0002 m.

particularly for the larger assumed value of s_c. *Dreybrodt* [1990], *Palmer* [1991], and *Groves and Howard* [1994a] provide more information on the effect of parameter variation on the time required for cave development in single-passage caves.

Discussion

In contrast to the highly selective passage enlargement that occurs early in cave network development under laminar flow, the transition to turbulent flow often results in more general passage enlargement, leading to various degrees of maze network development. The greatest maze development occurs with a combination of large initial passage diameter and high hydraulic gradient, with the passage diameter providing the greatest control. Hydraulic gradients greater than about 0.05 are required to have even modest maze development when initial effective passage diameter is about 0.001 m, but hydraulic gradients as low as 0.0003 result in strong maze development when initial passage diameters are about 0.01 m.

The general tendency for some maze development under turbulent flow conditions coupled with the very selective enlargement under laminar flow is just the opposite of the suggestion by *Curl* [1974] that all conduits should be competitive under laminar flow (thus forming mazes), and that passages successful in competition for flow would be limited to those in which turbulent flow was first achieved, thereby drastically increasing solution rates. This analysis was based upon earlier work [*Curl*, 1965] suggesting that dissolution rates are transport controlled, limited by the rate of $H_2CO_3^0$ diffusion to the mineral surface. Thus reaction rates would increase dramatically in the first conduit to reach turbulent flow due to turbulent mixing and diffusion control through a thin laminar sublayer. While there seems to be little disagreement that transport rates limit dissolution far from equilibrium ($pH < 4$), other results show that reaction rates can become limiting for higher concentrations [*Plummer and Wigley*, 1976; *Plummer et al.*, 1978, 1979; *Morse*, 1983; *White*, 1988; *Dreybrodt*, 1988, 1990; *Palmer*, 1991], and *Groves and Howard* [1994b] show that these high-order surface reaction rates become limiting under the near-saturation conditions that are likely to occur during early stages of passage development within the bulk of the aquifer.

Development of alternate pathways under conditions of turbulent flow depends on the ability of relatively undersaturated solutions to penetrate deeply into the fracture network and to produce a more even flow distribution among alternate flow paths in turbulent or mixed laminar and turbulent flow. Our results support two of the hypotheses suggested by *Palmer* [1975, 1991] for the development of network maze patterns:

1. These patterns occur when there is a network of large initial pathways. Large fractures (approximately 0.004 m or larger) might be formed by application or release of stresses by such processes as unloading, tectonic activity, or gravity sliding. In an analysis of 260 maze caves, *Palmer* [1975] found that most were associated with topographic settings favorable to unloading, including escarpments, residual hills, canyon walls (especially at or across bends), and regions subject to Pleistocene glaciation. Some maze caves were also found within the axes of anticlinal flexures.
2. Large hydraulic gradients and large maximum discharges favor the development of network maze patterns. Field evidence also suggests that maze cave formation occurs in response to episodic flooding of passages by recharge from discrete recharge points during intense rainfall or snowmelt. This can take place, for example, where the limestone received drainage from a large catchment of noncarbonate rocks. Passage constrictions as a result of collapse, sediment blockage, or insoluble beds can also contribute to steep gradients.

Aside from these situations the simulations indicate that any hydrogeologic setting promoting long-duration, turbulent phreatic flow of initially unsaturated water through limestone fractures is likely to result in some maze development. One such setting is regional artesian flow, as was suggested by *Tullis and Gries* [1938], *Deike* [1960], *Howard* [1963, 1964] and others (although *Palmer* [1975, 1991] doubts that artesian flow is a sufficient explanation for maze caves). In addition to flow strictly within a limestone, flow descending [*Palmer*, 1991] or ascending [*Bakalowicz et al.*, 1987; *Ford*, 1989; *Klimchouk*, 1991] into a limestone from overlying or underlying rocks may occur, either from a few discrete sources or as diffuse contributions (the latter case has not been simulated here). In addition to initial undersaturation, limestone dissolution in artesian flow may occur due to rising thermal waters [*Bakalowicz et al.*, 1987; *Ford*, 1989] and mixing of saturated flows equilibrated with different initial partial pressures of CO_2 (Mischungskorrosion) [*Bögli*, 1964; *Dreybrodt*, 1981; *Palmer*, 1991; *Ford*, 1989]. In addition, *Worthington* [1991] shows that variations in groundwater viscosity due to the geothermal heat gradient can influence patterns of flow and passage development. These processes are not considered here.

On the other hand, single-channel or branched patterns will be favored for conditions of cave development entirely via laminar flow (unlikely within large cave systems), initially tight fractures, and low hydraulic gradients. In addition, cave development via solution by underground, free-surface streams (vadose conditions) will likely also result in branched patterns. Such cave systems are likely to have started by shallow phreatic flow originating from a number of discrete sinkhole inputs, but have become vadose as passages enlarged and the piezometric surface is depressed. Several factors inhibit maze development by free-surface cave streams: (1) the development of free-surface streams depresses the water table, so that flow from tributary feeders occurs at high gradients and the sharing of groundwater among adjacent fractures that is largely responsible for maze passage development is discouraged; (2) as main passages cut downward by abrasion or dissolution, more slowly eroding tributary conduits develop steep gradients or enter as high-level springs, further concentrating flow into a dendritic pattern; and (3) introduction of sediment along the major subterranean streams may encourage sedimentation and flow blockage within adjacent solutionally enlarged fractures.

Acknowledgments. We would like to thank Deana Groves, Janet Herman, Carol Wicks, George Hornberger, Robert Ribando, and Robin Diederich with assistance in various aspects of this research. Financial support for the project was provided by the Cave Research Foundation, the University of Virginia, and the National Speleological Society.

References

Bakalowicz, M. J., D. C. Ford, T. E. Miller, A. N. Palmer, and M. V. Palmer, Thermal genesis of dissolution caves in the Black Hills, South Dakota, *Geol. Soc. Am. Bull.*, *99*, 729–738, 1987.

Bögli, A., Mischungskorrosion—Ein Beitrag zum Verkarstungsproblem, *Erdkunde*, *18*, 83–92, 1964.

Bretz, J. H., Vadose and phreatic features of limestone caverns, *J. Geol.*, *50*, 675–811, 1942.

Curl, R. L., Solution kinetics of calcite, paper presented at 4th International Congress of Speleology, Ljubljana, Slovenia, 1965.

Curl, R. L., Cave conduit competition: nonautonomous systems, in Proceedings of the Fourth Conference on Karst Geology and Hydrology, edited by H. W. Rauch and E. Werner, p. 109, W. Va. Geol. and Econ. Surv., Morgantown, 1974.

Davis, W. M., Origin of limestone caverns, *Geol. Soc. Am. Bull.*, *41*, 475–628, 1930.

Deike, G. H., III, Origin and geologic relations of Breathing Cave, Virginia, *Natl. Speleol. Soc. Bull.*, *22*, 30–42, 1960.

Dreybrodt, W., Mixing corrosion in $CaCO_3$-CO_2-H_2O systems and its role in the karstification of limestone areas, *Chem. Geol.*, *32*, 221–236, 1981.

Dreybrodt, W., *Processes in Karst Systems*, 288 pp., Springer-Verlag, New York, 1988.

Dreybrodt, W., The role of dissolution kinetics in the development of karst aquifers in limestone: A model simulation of karst evolution, *J. Geol.*, *98*, 639–655, 1990.

Ford, D. C., Features of the genesis of Jewel Cave and Wind Cave, Black Hills, South Dakota, *Natl. Speleol. Soc. Bull.*, *51*, 100–110, 1989.

Ford, D. C., and R. O. Ewers, The development of limestone cave systems in the dimensions of length and depth, *Can. J. Earth Sci.*, *15*, 1783–1798, 1978.

Ford, D. C., and P. W. Williams, *Karst Geomorphology and Hydrology*, 601 pp., Unwin Hyman, Boston, Mass., 1989.

Gnielinski, V., New equations for heat and mass transfer in turbulent pipe and channel flow, *Int. Chem. Eng.*, *16*, 359–368, 1976.

Groves, C. G., Early development of karst systems, Ph.D. dissertation, 253 pp., Dep. of Environ. Sci., Univ. of Va., Charlottesville, 1993.

Groves, C. G., and A. D. Howard, Minimum hydrochemical conditions allowing limestone cave development, *Water Resour. Res.*, *30*, 607–615, 1994a.

Groves, C. G., and A. D. Howard, Early development of karst systems, 1, Preferential flow path enlargement under laminar flow, *Water Resour. Res.*, *30*, 2837–2846, 1994b.

Howard, A. D., Processes of limestone cavern development, *Int. J. Speleol.*, *1*, 47–60, 1963.

Howard, A. D., A model for cavern development under artesian ground water flow, with special reference to the Black Hills, *Natl. Speleol. Soc. Bull.*, *26*, 7–16, 1964.

Jeppson, R. W., *Analysis of Flow in Pipe Networks*, 164 pp., Butterworth, Stoneham, Mass., 1976.

Klimchouk, A. B., Large maze caves in gypsum in the western Ukraine: Speleogenesis under artesian conditions, *Natl. Speleol. Soc. Bull.*, *53*, 71–82, 1991.

Morse, J. W., The kinetics of calcium carbonate dissolution and precipitation, *Rev. Mineral.*, *11*, 227–264, 1983.

Palmer, A. N., The origin of maze caves, *Natl. Speleol. Soc. Bull.*, *37*, 56–76, 1975.

Palmer, A. N., Geomorphic interpretation of karst features, in *Groundwater as a Geomorphic Agent*, edited by R. G. LaFleur, pp. 173–209, Allen and Unwin, Winchester, Mass., 1984.

Palmer, A. N., The origin and morphology of limestone caves, *Geol. Soc. Am. Bull.*, *103*, 1–21, 1991.

Plummer, L. N., and T. M. L. Wigley, The dissolution of calcite in CO_2 saturated solutions at 25°C and 1 atmosphere total pressure, *Geochim. Cosmochim. Acta*, *40*, 191–202, 1976.

Plummer, L. N., T. M. L. Wigley, and D. L. Parkhurst, The kinetics of calcite dissolution in CO_2-water systems at 5 to 60°C and 0.0 to 1.0 atm CO_2, *Am. J. Sci.*, *278*, 179–216, 1978.

Plummer, L. N., D. L. Parkhurst, and T. M. L. Wigley, Critical review of the kinetics of calcite dissolution and precipitation, in Chemical Modeling in Aqueous Systems, edited by E. A. Jenne, *Am. Chem. Soc. Symp. Ser.*, *93*, 537–573, 1979.

Powell, R. L., Joint patterns and solution channel evolution in Indiana, *Mem. Int. Assoc. Hydrogeol.*, *12*, 255–269, 1977.

Press, W. H., B. P. Flannery, S. A. Teukolsky, and W. T. Vetterling, *Numerical Recipes*, 818 pp., Cambridge University Press, New York, 1986.

Sasowsky, I. D., Evolution of the Appalachian highlands: Geochemistry, hydrogeology, cave sediment magnetostratigraphy and historical geomorphology of East Fork Obey River, Fentress County, Tennessee, Ph.D. dissertation, 174 pp., Dep. of Geosci., Pa. State Univ., University Park, 1992.

Tullis, E. L., and J. P. Gries, The Black Hills caves, *Black Hills Eng.*, *24*, 233–271, 1938.

White, W. B., Role of solution kinetics in the development of karst aquifers, *Mem. Int. Assoc. Hydrogeol.*, *12*, 503–517, 1977.

White, W. B., *Geomorphology and Hydrology of Karst Terrains*, 464 pp., Oxford University Press, New York, 1988.

White, W. B., and J. Longyear, Some limitations on speleo-genetic speculation imposed by the hydraulics of groundwater flow in limestone, *Nittany Grotto Newsl.*, *10*, 155–167, 1962.

Worthington, S. R. H., Karst hydrogeology of the Canadian Rocky Mountains, Ph.D. dissertation, 370 pp., Dep. of Geogr., McMaster Univ., Hamilton, Ont., Canada, 1991.

C. G. Groves, Center for Cave and Karst Studies, Department of Geography and Geology, Western Kentucky University, Bowling Green, KY 42101.

A. D. Howard, Department of Environmental Sciences, University of Virginia, Charlottesville, VA 22903.

(Received February 22, 1994; revised July 7, 1994;
accepted July 24, 1994.)